JACS
JOURNAL OF THE AMERICAN CHEMICAL SOCIETY

Communication

pubs.acs.org/JACS

Robust DNA-Functionalized Core/Shell Quantum Dots with Fluorescent Emission Spanning from UV−vis to Near-IR and Compatible with DNA-Directed Self-Assembly

Zhengtao Deng,[†] Anirban Samanta,[†] Jeanette Nangreave, Hao Yan,* and Yan Liu*

The Biodesign Institute and Department of Chemistry and Biochemistry, Arizona State University, Tempe, Arizona, 85287, United States

Supporting Information

ABSTRACT: The assembly and isolation of DNA oligonucleotide-functionalized gold nanoparticles (AuNPs) has become a well-developed technology that is based on the strong bonding interactions between gold and thiolated DNA. However, achieving DNA-functionalized semiconductor quantum dots (QDs) that are robust enough to withstand precipitation at high temperature and ionic strength through simple attachment of modified DNA to the QD surface remains a challenge. We report the synthesis of stable core/shell (1−20 monolayers) QD−DNA conjugates in which the end of the phosphorothiolated oligonucleotide (5−10 nucleotides) is "embedded" within the shell of the QD. These reliable QD−DNA conjugates exhibit excellent chemical and photonic stability, colloidal stability over a wide pH range (4−12) and at high salt concentrations (>100 mM Na^+ or Mg^{2+}), bright fluorescence emission with quantum yields of up to 70%, and broad spectral tunability with emission ranging from the UV to the NIR (360−800 nm).

Organizing inorganic nanoparticles (NPs) with nanoscale precision is of great interest for energy, nanophotonics, and nanobiotechnology applications.[1] One of the most promising approaches for the fully programmable self-assembly of NPs, DNA nanotechnology, relies on Watson−Crick base-pairing interactions between DNA-functionalized NPs and underlying DNA nanoscaffolds.[2] DNA-directed self-assembly of oligonucleotide-functionalized gold NPs (AuNPs) was first introduced by Mirkin[3] and Alivisatos[4] in 1996. Since then, the process of attaching thiolated oligonucleotides to citrate-stabilized AuNPs through successive salt aging has been well-developed.[5] These stable DNA−AuNP conjugates have enabled the DNA-directed self-assembly of one-dimensional (1D) AuNP self-similar chains and arrays,[6a,b] two-dimensional (2D) AuNP superlattice sheets,[6c] three-dimensional (3D) AuNP tubes,[6d] AuNP superlattice crystals,[6e] and even chiral plasmonic AuNP nanostructures with tailored optical responses.[6f]

However, less progress in organizing semiconductor NPs or quantum dots (QDs) into architectures with interesting fluorescence properties has been made. To facilitate DNA-directed assembly of semiconductor QDs and achieve reliable architectures, the QDs should exhibit the following properties: (1) High chemical and photonic stability. The QDs should be highly resistant to chemical degradation and photobleaching during assembly of the underlying DNA nanoscaffolds, as the annealing process involves relatively high temperatures and ion concentrations; this requires the use of core/shell QDs. (2) Strong binding affinity between the DNA oligonucleotides and the QDs. The chemically modified oligonucleotides should not detach from the QD surface while in solution; thus, conventional thiolated oligonucleotide binding strategies are not adequate. (3) High colloidal stability over a wide range of buffer conditions. The chemically modified oligonucleotides should not precipitate or aggregate at high salt concentrations (>100 mM Na^+ or Mg^{2+}) and should be stable at a variety of pHs. (4) High fluorescence quantum efficiency (>50%). This is important when the QDs are used as fluorescent markers for molecular detection or monitoring of biological processes at the single-particle level. (5) High spectral tunability to achieve a wide range of QD emissions. This is critical in applications such as biolabeling, light manipulation, and controlled energy transfer.

Recently, DNA−protein interactions have been used to arrange QDs on DNA tile arrays and origami. In 2008, we used biotinylated DNA tile arrays to direct the assembly of streptavidin-conjugated CdSe/ZnS core/shell QDs into well-defined periodic patterns.[7a] In 2010, Bui et al.[7b] used biotinylated DNA origami nanotubes to assemble streptavidin-conjugated CdSe/ZnS QDs into arrays. In 2012, Ko et al.[7c] used biotinylated DNA origami to assemble streptavidin-functionalized QDs. Unfortunately, the complexity of structures that can be formed by this method is limited, as the biotin−streptavidin interaction is not information-bearing.

Alternatively, QD−DNA conjugates can be designed to bind directly to an underlying DNA nanostructure through sequence-specific Watson−Crick base pairing, providing a significant increase in the level of structural complexity that can be achieved. Several conjugation strategies for attaching DNA oligonucleotides to the surface of QDs have been developed. Mirkin[8a] reported the attachment of thiol-modified (3′-propylthiol or 5′-hexylthiol) single-stranded DNA (ssDNA) to the surface of CdSe/ZnS QDs, similar to ssDNA−AuNP conjugates. We reported the attachment of thiol-modified ssDNA to the surface of CdSe/ZnS core/shell QDs, where the conjugation occurred during a one-step core/shell formation process.[8b] Recently, Kelley[8c] reported a synthetic route to produce phosphorothiolated phosphorodiester DNA (ps-po-DNA)-functionalized

Received: August 15, 2012
Published: October 5, 2012

   dx.doi.org/10.1021/ja3081023 | J. Am. Chem. Soc. 2012, 134, 17424−17427

CdTe QDs, but these core-only QDs without shells had a low quantum yield (<50%). The above QD−DNA conjugates were less stable than their AuNP−DNA counterparts under similar buffer conditions. This is the case because Au−S bonds (ΔH = 418 kJ/mol) are much stronger than Au−O bonds (ΔH = 221.8 kJ/mol), enabling the thiolated DNA to displace the original citrate ligand on the AuNP surface and form stable Au−DNA conjugation, whereas the strengths of Cd−S (ΔH = 208.4 kJ/mol) and Zn−S bonds (ΔH = 205 kJ/mol) are similar to those of Cd−O (ΔH = 235.6 kJ/mol) and Zn−O bonds (ΔH = 159 kJ/mol),[9] allowing these thiol ligands on the QD surface to be displaced by other ionic species present in the aqueous buffer.

Herein we report a new strategy to achieve robust DNA-functionalized core/shell QDs that satisfy all five requirements for DNA-directed self-assembly listed above. Our strategy for forming these QD−DNA conjugates (Figure 1) takes advantage

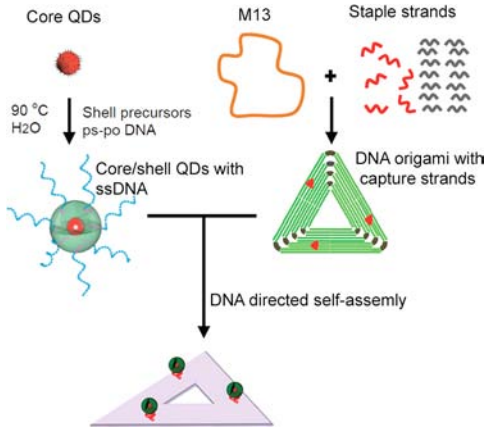

Figure 1. DNA functionalization of core/shell QDs and organization by self-assembled DNA origami. Core/shell QDs are functionalized with oligonucleotides during shell growth in aqueous solution at 90 °C for 20−120 min. The resulting core/thick-shell QDs are chemically, photonically, and colloidally stable and display PL quantum yields of up to 70% and broad spectral tunability from the UV to the NIR. The DNA oligonucleotides contain phosphorothiolated (ps) domains (5−10 nucleotides; shown in violet) for incorporation of the DNA directly into the outer QD shells and a typical phosphodiester (po) backbone (blue) for recognition by DNA capture probes within origami structures. The QD core (red) can be synthesized in aqueous solution or an organic solvent. The shells (green) are CdS or ZnS. Simultaneously, self-assembled DNA origami structures were synthesized by thermal annealing of M13 DNA with staple strands (gray) and capture strands (red). Finally, hybridization of the recognition domains of the QD−DNA conjugates to complementary capture strands displayed on the surface of the DNA origami yields higher-order architectures.

of chimeric ps-po-ssDNA strands that are directly inserted within a thick CdS or ZnS QD shell during its synthesis over the core. This synthetic route results in core/shell QD−DNA conjugates that are chemically, photonically, and colloidally stable as well as highly fluorescent [with photoluminescence (PL) quantum yields of up to 70%] for a wide range of semiconductor materials with tunable fluorescent emissions spanning from the UV to the NIR (360−800 nm). We also demonstrate the organization of these QD−DNA conjugates by complementary base pairing to triangular- and rectangular-shaped DNA origami structures.

The synthesis proceeded as follows: first, water-soluble mercaptopropionic acid (MPA)-capped CdTe core QDs were encapsulated with thick CdS shells in the presence of ps-po-ssDNA [for details, see pages S3−S12 and Figures S1−S9 in the Supporting Information (SI)]. The magic-sized MPA-capped CdTe nanocrystals (1.6 nm diameter with peak PL at 480 nm) were synthesized as described previously.[10] In a typical reaction, an aliquot of CdTe core QDs was purified and redissolved in 100 μL of nanopure water. Prescribed amounts of Cd^{2+}−MPA complex (the precursor of both Cd and S for CdS shell growth) and ps-po-ssDNA (the surface ligand) were added to the core mixture. The ps-po-ssDNA oligonucleotides (5′-T28-G5-ps-3′) contained a stretch of five consecutive G residues followed by five consecutive ps backbone modifications and 28 unmodified T residues linked by conventional phosphodiester bonds. The pH was adjusted to 12, and the mixture was heated at 90 °C for 70 min. During this time, the Cd^{2+}−MPA complex slowly decomposed, and a CdS shell of particular thickness was formed around the CdTe core. The five S atoms in the ps domain of the DNA were "inserted" into the CdS shell during its formation, while most (if not all) of the poly-T domain extended away from the surface of the shell and was available for hybridization to the complementary DNA within the underlying DNA nanostructure. As we reported previously,[10] at this relatively mild temperature the monolayer-by-monolayer formation of the CdS shell is fully controlled by the slow decomposition of the Cd^{2+}−MPA complex, and the shell thickness is determined by the total reaction time. We observed that seven CdS shell monolayers formed in 70 min, so the estimated synthesis time was 10 min/monolayer. In view of the relatively low rate of growth, the S atoms in the ps domains of the oligonucleotides had ample opportunity to bond to the Cd atoms and were readily incorporated into the CdS shell. From the UV−vis absorption spectra, the number of ssDNA on one QD was estimated to be 9 (see Figure S9).

The resulting core/shell CdTe/CdS QD−DNA conjugates had an estimated diameter of 6.5 nm, corresponding to a seven-monolayer CdS (7CdS) shell, with a band-edge emission maximum at 672 nm and a PL quantum yield of 70%. The observed ∼200 nm red shift of the emission peak is assigned to quasi-type-II QDs.[12] Transmission electron microscopy (TEM) and high-resolution TEM (HRTEM) images revealed that the QD−DNA conjugates were monodispersed, single-crystalline particles (Figure 2a). The purified thick-shell QD−DNA conjugates were found to be stable under a variety of buffer conditions, including 1× PBS buffer at pH 4.0, 7.0, and 10.0; 1× TAE−Mg^{2+} buffer; 1× TBE−Mg^{2+} buffer; and 10× TAE−Mg^{2+} buffer (125 mM Mg^{2+}) (Figure 2c). Thus, our QD−DNA conjugates are colloidally stable over a wide pH range (4−12) at high salt concentrations (>100 mM Na^+ or Mg^{2+}).

These CdTe/7CdS QD−DNA conjugates were subsequently assembled at precise positions on DNA origami structures via hybridization to complementary poly-A capture probes extending from the origami surface (three capture probes per QD−DNA). We demonstrated the organization of three or two QD−DNA conjugates on triangular or rectangular DNA origami, respectively (Figure 2d−g). Atomic force microscopy (AFM) and scanning TEM (STEM) confirmed that >95% of the triangular DNA origami structures displayed three QDs, one on each arm (Figure 2d,f), and that 90% of the rectangular origami structures displayed two QD−DNA conjugates, one each at opposite corners (Figure 2e,g), as prescribed by the design (for design details and additional images, see SI pages S29−S45 and Figures S24−S26). The AFM height profiles showed that the QD−DNA conjugates had a narrow size range (6−7 nm).

We also synthesized thick-shell CdSe/CdS QD−DNA conjugates containing 20-monolayer CdS (20CdS) shells. As

dx.doi.org/10.1021/ja3081023 | J. Am. Chem. Soc. 2012, 134, 17424−17427

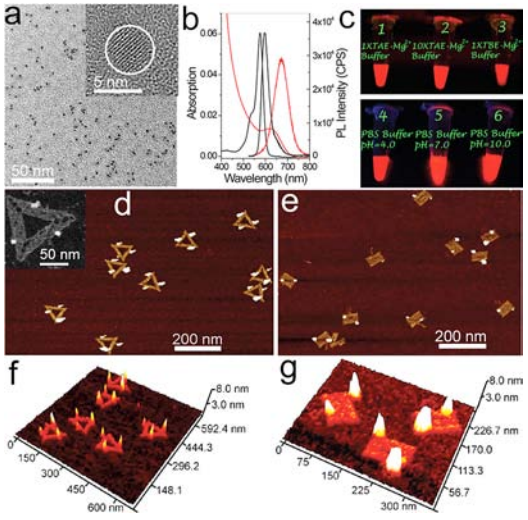

Figure 2. DNA-functionalized CdTe/7CdS core/shell QDs with MPA-capped magic-sized CdTe cores and emission at 672 nm. (a) TEM and HRTEM images of the QD−DNA conjugates. (b) UV−vis absorption and PL emission spectra of the conjugates (red) and the reference dye rhodamine 101 (black) for PL quantum yield measurements. Comparison with the PL intensity of the reference dye revealed that the QD−DNA conjugates displayed a quantum yield of 70%. (c) Photographs of the QDs illuminated with a 365 nm UV lamp in several different buffers: (1) 1× TAE−Mg^{2+}; (2) 10× TAE−Mg^{2+}; (3) 1× TBE−Mg^{2+}; (4−6) PBS buffers at pH 4, 7, and 10, respectively. (d−g) AFM images and height profiles of the CdTe/CdS QDs organized by triangular (three QDs total, one QD per arm) and rectangular (two QDs total, in opposite corners) DNA origami. The inset in (d) is a STEM image of CdSe/7CdS QD−DNA conjugates assembled on triangular DNA origami, whose triangular shape was made visible by negative staining with uranyl formate.

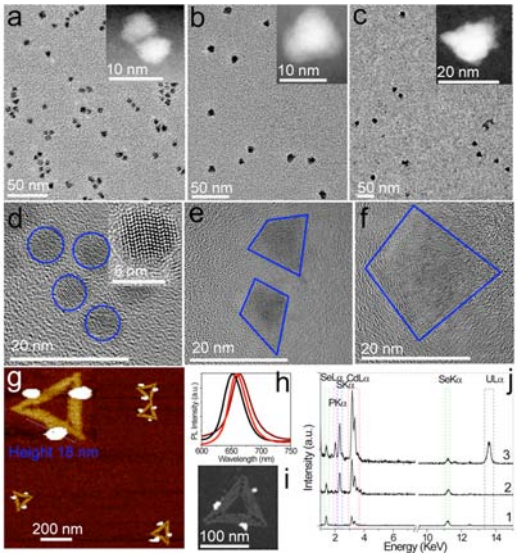

Figure 3. Characterization of various stages during the synthesis of CdSe/20CdS QD−DNA conjugates. (a−c) TEM and (insets) STEM images and (d−f) HRTEM images of (a, d) OLA-capped CdSe core QDs (spherical, 6 nm in diameter), (b, e) core/shell CdSe/9CdS QDs (tetrahedral, 12 nm in length), and (c, f) thick-shell CdSe/20CdS QD−DNA conjugates (tetrahedral, 18 nm in length). (g) AFM image and (inset) height profile and (i) STEM image of CdTe/20CdS QD−DNA conjugates organized by triangular DNA origami. (h) PL and (j) EDS spectra of CdSe QDs (black, "1"), CdSe/9CdS QDs (red, "2") and CdTe/20CdS QD−DNA conjugates (wine, "3").

reported by Hollingsworth[11a] and Dubertret,[11b] "giant"-shell or thick-shell QDs are more chemically stable and exhibit reduced blinking behavior at the single-particle level. Thick-shell QDs have been obtained by the successive ionic layer adsorption and reaction (SILAR) method,[11] which requires high temperatures (240 °C) and a growth process in an organic solvent. Here we developed a new method to achieve thick-shell CdSe/20CdS QDs at lower temperatures (90 °C) in aqueous solution. More significantly, we incorporated the ssDNA within the shell itself during the encapsulation process. First, oleic acid (OLA)-capped CdSe core QDs (6 nm diameter) were synthesized in paraffin liquid at 320 °C (Figure 3a,d; for details, see SI pages S13−S21 and Figures S10−S17).[11c] The OLA-capped CdSe cores had diameters of ∼6.0 nm and fluorescence emission at 650 nm. Next, nine-monolayer CdS shells were deposited on the CdSe cores in aqueous solution at 90 °C with MPA as the capping ligand. After the ligand exchange and CdS shell growth, the tetrahedral-shaped MPA-capped QDs exhibited emission at 660 nm. The approximate length of these tetrahedral-shaped QDs was 12 nm (Figure 3b,e). Finally, additional shells were incorporated on the QDs in the presence of ps-po-ssDNA. The resulting DNA oligonucleotide-functionalized thick-shell CdSe/20CdS QDs emitted at 663 nm. The length of the QD−DNA conjugates increased to 18 nm (Figure 3c,f). The relatively small size of the PL red shift upon shell growth was due to the large core size of these core/shell QDs (6 nm diameter), as small-core (3 nm diameter) CdSe QDs encapsulated with a thick shell showed a PL red shift of 70 nm (from 565 to 635 nm; Figure S10). This may be a strain-induced PL shift.[11d]

We demonstrated that these robust, thick-shell QD−DNA conjugates are readily organized by addressable DNA origami structures to form discrete, well-ordered nanoarchitectures. In addition, DNA origami are an ideal platform to confirm the successful DNA functionalization of the QDs, which is more straightforward and reliable than the previous QD−DNA/dye FRET method.[8b] As demonstrated in Figure 3j, energy-dispersive X-ray spectroscopy (EDS) spectra of the self-assembled origami nanostructures revealed the presence of Cd, Se, S, and P from the CdSe/20CdS QD−DNA conjugates.

This strategy is quite versatile and can be applied to QDs composed of other semiconductor materials (Figure 4). For example, we found that ZnS shells could be deposited on a variety of different core materials using the same strategy. Using a water-soluble ZnSe core,[12a] we produced ZnSe/4ZnS QD−DNA conjugates displaying UV emission at 360 nm (Figure 4; for details, see SI pages S22−S28 and Figures S18−S23). Using OLA-capped CdS or quaternary-alloy ZnCdSSe QD cores,[12b] we synthesized CdS/4ZnS QD−DNA conjugates with blue emission at 425 nm and ZnCdSSe/4ZnS QD−DNA conjugates with green emission at 510 nm, respectively. Furthermore, we produced CdTe/4ZnS QD−DNA conjugates with yellow emission at 555 nm. Finally, we used magic-sized CdTe core QDs to synthesize a series of DNA-functionalized QDs, including CdTe/2CdS, CdTe/4CdS, and thick-shell CdTe/10CdS and CdTe/13CdS QDs with emission maxima in the orange, red, and NIR at 575, 610, 740, and 800 nm, respectively. The organization of each of these QD−DNA conjugates by DNA origami is shown in Figure 4. The AFM height profiles of the particles corresponded well to the sizes measured using TEM.

Since CdS and ZnS are wide-band-gap semiconductor materials that are generally used in QD shells, it is reasonable to expect that many other core/shell QDs with various core

dx.doi.org/10.1021/ja3081023 | J. Am. Chem. Soc. 2012, 134, 17424−17427

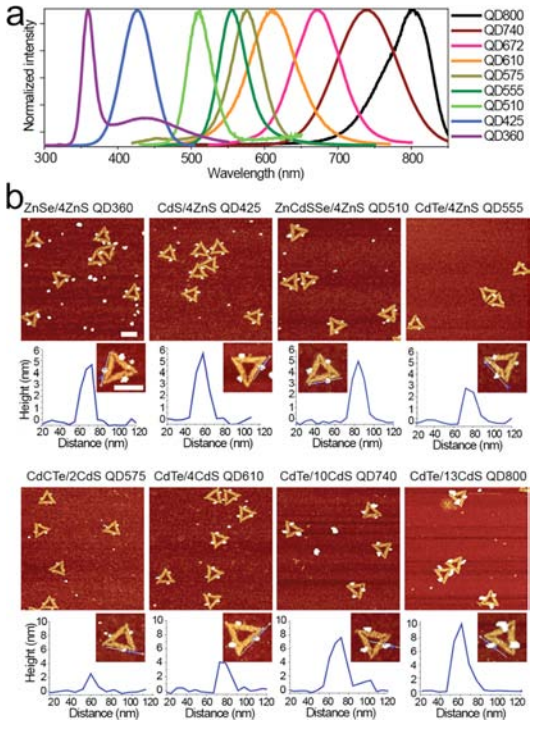

Figure 4. (a) Fluorescence spectra of a series of DNA-functionalized core/shell QDs with tunable emission from the UV to the NIR. (b) Zoomed-out and -in AFM images and corresponding height profiles of QD−DNA/DNA origami structures. The conjugates have the following emissions and compositions: UV-emitting (360 nm) ZnSe/4ZnS QDs; blue-emitting (425 nm) ZnSe/4ZnS QDs; green-emitting (510 nm) ZnCdSSe/4ZnS QDs; yellow-emitting (555 nm) CdTe/2ZnS QDs; yellow-emitting (575 nm) CdTe/2CdS; orange-emitting (610 nm) CdTe/4CdS; NIR-emitting (740 nm) CdTe/8CdS; and NIR-emitting (800 nm) CdTe/13CdS, respectively. The scale bars are 100 nm.

compositions can be synthesized, such as binary PbS, InP, and InAs QDs for IR emission; doped ZnSe:Mn QDs; ternary-alloy CuInSe and ZnCdSe QDs; quaternary-alloy CuInSSe QDs; and so on. All of these should be compatible with the oligonucleotide functionalization strategy reported here.

In summary, we have developed a simple and efficient method to synthesize robust core/shell QD−DNA conjugates that can withstand the conditions necessary for DNA-directed assembly. In contrast to QD functionalization strategies in which the DNA ligands are simply attached to the QD surface, our method embeds the DNA within the shell itself, providing greater stabilization. Our strategy can be used with a wide variety of semiconductor materials displaying PL emission ranging from the UV to the NIR. Also, discrete numbers of QD−DNA conjugates can be organized by DNA origami nanostructures, an essential component of hierarchical NP assembly efforts. This work will facilitate the construction of discrete, multicomponent semiconductor or semiconductor−metal hybrid nanostructures for energy, nanophotonics, and biosensing applications.

■ ASSOCIATED CONTENT

Ⓢ Supporting Information

Experimental details and Figures S1−S26. This material is available free of charge via the Internet at http://pubs.acs.org.

■ AUTHOR INFORMATION

Corresponding Author

hao.yan@asu.edu; yan_liu@asu.edu

Author Contributions

†Z.D. and A.S. contributed equally.

Notes

The authors declare no competing financial interest.

■ ACKNOWLEDGMENTS

We thank ONR, DOE, ARO, NSF, and NIH for support of Y.L. and H.Y., who were also supported as part of the Center for Bio-Inspired Solar Fuel Production, an Energy Frontier Research Center funded by DOE BES under Award DE-SC0001016. Z.D. was supported by a grant from DOD-ONR.

■ REFERENCES

(1) (a) Service, R. F. *Science* **2005**, *309*, 95. (b) Srivastava, S.; Santos, A.; Critchley, K.; Kim, K. S.; Podsiadlo, P.; Sun, K.; Lee, J.; Xu, C. L.; Lilly, G. D.; Glotzer, S. C.; Kotov, N. A. *Science* **2010**, *327*, 1355. (c) Liu, Y. *Nat. Nanotechnol.* **2011**, *6*, 463.

(2) (a) Seeman, N. C. *Nature* **2003**, *421*, 427. (b) Pinheiro, A. V.; Han, D. R.; Shih, W. M.; Yan, H. *Nat. Nanotechnol.* **2011**, *6*, 763. (c) Tan, S. J.; Campolongo, M. J.; Luo, D.; Cheng, W. L. *Nat. Nanotechnol.* **2011**, *6*, 268.

(3) Mirkin, C. A.; Letsinger, R. L.; Mucic, R. C.; Storhoff, J. J. *Nature* **1996**, *382*, 607.

(4) Alivisatos, A. P.; Johnsson, K. P.; Peng, X. G.; Wilson, T. E.; Loweth, C. J.; Bruchez, M. P.; Schultz, P. G. *Nature* **1996**, *382*, 609.

(5) (a) Hurst, S. J.; Lytton-Jean, A. K. R.; Mirkin, C. A. *Anal. Chem.* **2006**, *78*, 8313. (b) Cutler, J. I.; Auyeung, E.; Mirkin, C. A. *J. Am. Chem. Soc.* **2012**, *134*, 1376. (c) Elghanian, R.; Storhoff, J. J.; Mucic, R. C.; Letsinger, R. L.; Mirkin, C. A. *Science* **1997**, *277*, 1078.

(6) (a) Zhang, J. P.; Liu, Y.; Ke, Y. G.; Yan, H. *Nano Lett.* **2006**, *6*, 248. (b) Ding, B. Q.; Deng, Z. T.; Yan, H.; Cabrini, S.; Zuckermann, R. N.; Bokor, J. *J. Am. Chem. Soc.* **2010**, *132*, 3248. (c) Cheng, W. L.; Campolongo, M. J.; Cha, J. J.; Tan, S. J.; Umbach, C. C.; Muller, D. A.; Luo, D. *Nat. Mater.* **2009**, *8*, 519. (d) Sharma, J.; Chhabra, R.; Cheng, A.; Brownell, J.; Liu, Y.; Yan, H. *Science* **2009**, *323*, 112. (e) Macfarlane, R. J.; Lee, B.; Jones, M. R.; Harris, N.; Schatz, G. C.; Mirkin, C. A. *Science* **2011**, *334*, 204. (f) Kuzyk, A.; Schreiber, R.; Fan, Z. Y.; Pardatscher, G.; Roller, E. M.; Hogele, A.; Simmel, F. C.; Govorov, A. O.; Liedl, T. *Nature* **2012**, *483*, 311.

(7) (a) Sharma, J.; Ke, Y. G.; Lin, C. X.; Chhabra, R.; Wang, Q. B.; Nangreave, J.; Liu, Y.; Yan, H. *Angew. Chem., Int. Ed.* **2008**, *47*, 5157. (b) Bui, H.; Onodera, C.; Kidwell, C.; Tan, Y.; Graugnard, E.; Kuang, W.; Lee, J.; Knowlton, W. B.; Yurke, B.; Hughes, W. L. *Nano Lett.* **2010**, *10*, 3367. (c) Ko, S. H.; Gallatin, G. M.; Liddle, J. A. *Adv. Funct. Mater.* **2012**, *22*, 1015.

(8) (a) Mitchell, G. P.; Mirkin, C. A.; Letsinger, R. L. *J. Am. Chem. Soc.* **1999**, *121*, 8122. (b) Wang, Q. B.; Liu, Y.; Ke, Y. G.; Yan, H. *Angew. Chem., Int. Ed.* **2008**, *47*, 316. (c) Tikhomirov, G.; Hoogland, S.; Lee, P. E.; Fischer, A.; Sargent, E. H.; Kelley, S. O. *Nat. Nanotechnol.* **2011**, *6*, 485.

(9) *CRC Handbook of Chemistry and Physics*, 82nd ed.; Lide, D. R., Ed.; CRC Press: Boca Raton, FL, 2001.

(10) Deng, Z. T.; Schulz, O.; Lin, S.; Ding, B. Q.; Liu, X. W.; Wei, X. X.; Ros, R.; Yan, H.; Liu, Y. *J. Am. Chem. Soc.* **2010**, *132*, 5592.

(11) (a) Chen, Y.; Vela, J.; Htoon, H.; Casson, J. L.; Werder, D. J.; Bussian, D. A.; Klimov, V. I.; Hollingsworth, J. A. *J. Am. Chem. Soc.* **2008**, *130*, 5026. (b) Mahler, B.; Spinicelli, P.; Buil, S.; Quelin, X.; Hermier, J. P.; Dubertret, B. *Nat. Mater.* **2008**, *7*, 659. (c) Deng, Z.; Cao, L.; Tang, F.; Zou, B. *J. Phys. Chem. B* **2005**, *109*, 16671. (d) Smith, A. M.; Mohs, A. M.; Nie, S. *Nat. Nanotechnol.* **2009**, *4*, 56.

(12) (a) Deng, Z. T.; Lie, F. L.; Shen, S. Y.; Ghosh, I.; Mansuripur, M.; Muscat, A. J. *Langmuir* **2009**, *25*, 434. (b) Deng, Z. T.; Yan, H.; Liu, Y. *J. Am. Chem. Soc.* **2009**, *131*, 17744.